

# Monolithic Neat Graphene Oxide Aerogel for Efficient Catalysis of S → O Acetyl Migration

Li Peng,<sup>†</sup> Yaochen Zheng,<sup>†,‡</sup> Jiachen Li,<sup>†</sup> Yu Jin,<sup>†</sup> and Chao Gao<sup>\*,†</sup>

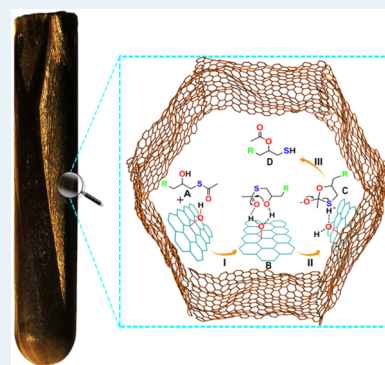
<sup>†</sup>MOE Key Laboratory of Macromolecular Synthesis and Functionalization, Department of Polymer Science and Engineering, Zhejiang University, 38 Zheda Road, Hangzhou 310027, People's Republic of China

<sup>‡</sup>College of Chemistry and Chemical Engineering, Yantai University, 30 Qingquan Road, Yantai, 264005, People's Republic of China

## S Supporting Information

**ABSTRACT:** Graphene oxide (GO) is highly attractive for catalysis because of its large specific surface area and rich chemical structures. However, it has generally been used as a catalyst carrier. Here, we designed a three-dimensional monolith of neat GO aerogel as a fixed-bed carbocatalyst used in the reaction of S → O acetyl migration for the synthesis of thiol compounds, showing the merits of ultrafast catalytic speed (5–8 h), high selectivity (100%), high yields (near 100%), easy isolation of products, and long-life recyclability (>18 times). Particularly, we achieved for the first time thiol compounds containing functional groups of halogen and hydroxyl, which cannot be synthesized using other currently reported catalysts. Control experiments demonstrated that the efficient catalysis mechanism is mainly attributed to the protonic functional groups, ultralarge size, and unpaired electrons of GO, as well as the “cage effect” at nanoscale confined spaces of aerogel cells.

**KEYWORDS:** carbocatalyst, graphene oxide, aerogel, fixed-bed, acetyl migration, thiol compound



## INTRODUCTION

Carbocatalysts are a convenient alternative for reducing the dependency on transition metal catalysts because of their sustainability and low-cost facial preparation.<sup>1</sup> As excellent candidates for carbocatalysts, graphene oxide (GO) and its derivatives<sup>2</sup> have been explored in the fields of photocatalysis,<sup>3</sup> electrocatalysis,<sup>4</sup> and organic reaction catalysis<sup>5</sup> because of their large specific surface area (SSA); conjugated domains; and abundant active sites, such as acidic and basic sites, debris,<sup>6</sup> holes and defects, unpaired  $\pi$  electrons of carbon,<sup>7</sup> and armchair and zigzag edges. In this regard, GO mainly plays three roles: catalyst carrier,<sup>8</sup> catalytic reagent,<sup>9</sup> and catalyst. In such reactions, GO is generally dispersed in solvents. After reaction, the product needs to be isolated from GO by a tedious centrifugation or filtration process, leading to low purity and yields.<sup>10</sup>

To resolve such a problem, GO or chemically converted graphene (CCG) can be assembled into a fixed bed. In 2010, the first GO assembled 3D fixed bed was prepared successfully by Wang and co-workers as the catalyst carrier for the Heck reaction.<sup>8</sup> In 2011, Liu's group used GO foam as the catalytic reagent to transform SO<sub>2</sub> into SO<sub>3</sub> at room temperature,<sup>11</sup> in which GO was reduced simultaneously and, thus, could not be recycled. In 2012, Loh's group prepared fixed bed, metallic catalysts deposited on CCG aerogel for oxidative coupling of amines.<sup>8b</sup> To date, a fixed bed carbocatalyst of neat GO or CCG has not been accessed.

Compared with metallic or inorganic catalysts, carbocatalyst is portable, low-cost, and tolerant of acids or bases. However,

successful catalytic reactions based on carbocatalysts have been quite limited, further explorations of new catalytic reactions are required. In this regard, achieving thiol compounds is of particular significance because of the emerging of thiol-click chemistry and thiol-based biological chemistry.<sup>12</sup> Various methods have been tried to synthesize thiol compounds using a variety of sulfur resources.<sup>13</sup> However, the persistent challenges of multistep reactions, relatively low yields, harsh conditions, and sulfide/disulfide byproducts have not been solved.<sup>14</sup> In 1942, Sjöberg first reported the S → O acetyl migration reaction to prepare thiol compounds catalyzed by a weak base (e.g., Na<sub>2</sub>CO<sub>3</sub> and pyridine) and weak acids (e.g., AcOH),<sup>15</sup> but the efficiency was extremely low (e.g., 8 h 45% conversion for Na<sub>2</sub>CO<sub>3</sub> catalyst at 0 °C, 13 h 18.5% conversion at 100 °C for AcOH catalyst). Following catalyses using triethylamine (TEA) and silica as catalysts were explored, but the purification step was still quite tedious.<sup>16</sup> The alkaline catalyst has inherent shortcomings, such as inevitable side reactions (e.g., formation of S–S) and no tolerance of molecules with specific functional groups, such as –Cl, –Br, –F, and –OH.

Here, we have designed a 3D monolith of neat GO aerogel as the carbocatalyst and catalyzed the S → O acetyl migration with an ultrahigh catalytic performance. The macroscopic GO aerogel (mGOa) is constructed of numerous microcells that

Received: February 4, 2015

Revised: April 20, 2015

Published: April 22, 2015

play roles of both catalyst and reactor (coined as catareactor). The reaction of  $S \rightarrow O$  acetyl migration demonstrated the ultrahigh catalytic activity and long-life recyclability (>18 times) of the macroscopic catareactors, readily giving rise to a series of thiol compounds with yields of 100%. Particularly, for the first time, we achieved thiol compounds containing functional groups of halogen and hydroxyl, which cannot be synthesized using other currently reported catalysts. Such catareactor-constructed mGOa not only opens the door for the design of novel catalytic reactors with merits of high efficiency, long-life recyclability, and easy separation, but also paves the way for laboratory, even industrial, synthesis of versatile thiol compounds.

## EXPERIMENTAL SECTION

**Catalyst Preparation. Preparation of Graphene Oxide (GO).** GO was purchased from C6G6 ([www.C6g6.com](http://www.C6g6.com)).<sup>17</sup> It was washed with deionized water more than 20 times and extensively dialyzed in a dialysis bag for 3 days against water to ensure the complete removal of residual metallic impurities.

**Preparation of mGOa.** The GO aqueous solution was used directly to fabricate mGOa in chromatographic columns via the “sol-cryo” method previously established by our group.<sup>18</sup> The GO solution was centrifuged (15 000 rpm for 4 h) to get a concentration of 25 mg/mL. Then the GO was loaded into the chromatographic column (Figure 1a); dried by freeze-drying

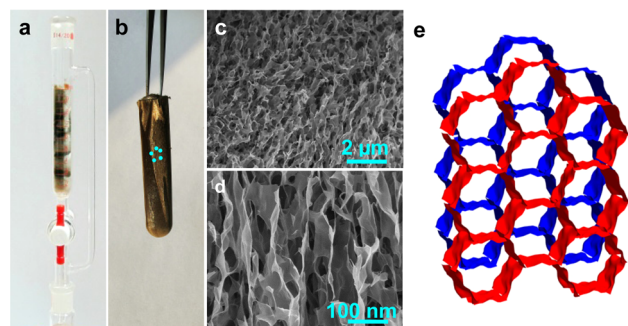


**Figure 1.** mGOa catareactors (a, b), SEM images of mGOa (c, d), and cartoon of cells in the mGOa (e).

for 2 days; and finally, resulted in a fixed-bed catalyst of neat GO aerogel (Figure 1b). The GO sheet-constructed cells were applied directly as catareactors without any postmodification and extra catalyst loading.

**$S \rightarrow O$  Acetyl Migration Reaction Catalyzed by mGOa.** The  $\beta$ -hydroxythioacetates were derived from the thiol–epoxy reactions between epoxy compounds and thioacetic acid in water or chloroform. Subsequently, the resulting latent thiol compounds were diluted with ethyl acetate, and slowly dropped into the mGOa fixed bed column. After standing for 5–8 h at rt, ethyl acetate was added into the column to elute the products, giving rise to  $\beta$ -acetate thiols. (See S3, Supporting Information, for further details.)

## RESULTS AND DISCUSSION

**Characterization of GO and mGOa.** The resulting GO (pH = 5 at a concentration of 1 mg/mL) has almost no metallic impurities (Mn 25 ppb; Fe 9 ppb; and Co, Cu, Pb, etc. below the detection limit) by inductively coupled plasma mass spectrometry (ICP-MS) analysis. The measurements of scanning electron microscopy (SEM) and atomic force

microscopy (AFM) showed that the prepared GO had an average lateral size of 12  $\mu\text{m}$  and thickness of 0.9 nm, confirming the single-layer nature of GO (S2 and Figure S1, Supporting Information).

The as-prepared mGOa fixed bed can be removed by a pair of tweezers, implying it is robust enough to be free-standing (Figure 1b). SEM images show that the mGOa has an interconnected 3D porous network (Figure 1c, d). The size of the continuous pores ranged from several nanometers to hundreds of nanometers, and the pore walls consist of 1–3 layers of GO sheets, which is verified by its high SSA (842  $\text{m}^2/\text{g}$ ) (Figure S2, Supporting Information). The partial overlapping or coalescing of the flexible GO sheets resulted in the formation of physical mechanical integrity.<sup>18</sup> Notably, such a fixed bed reactor is an integral monolith in appearance, and it is built with interconnected microcells that are favorable to efficient catalysis without stirring, so it is different from both conventional reactors that are dispersed in solvents and normal fixed bed reactors filled with individual solid state catalyst particles.<sup>19</sup>

**$S \rightarrow O$  Acetyl Migration Reaction Catalyzed in the Fixed Bed of mGOa.** The mGOa was used to catalyze the  $S \rightarrow O$  acetyl migration reaction using a variety of commercial epoxy compounds from 1a to 14a, shown in Table 1. The products (1c–14c) were determined by  $^1\text{H}$  NMR,  $^{13}\text{C}$  NMR, gas chromatography–mass spectrometry, and FTIR (Figure 2A, B; Figures S3–S37, Supporting Information). As shown in the  $^1\text{H}$  NMR (Figure 2A) results, new peaks of d' ( $\delta$ , 1.48 ppm) and e' ( $\delta$ , 2.13 ppm) appear, and peak d ( $\delta$ , 2.38 ppm) fades away, verifying the success of  $S \rightarrow O$  intramolecular acetyl migration. This result was also confirmed by the formation of  $-\text{SH}$  (7c) and the disappearing of  $-\text{OH}$  (7b) in the FTIR spectra (Figure 2B). In addition, no byproducts (e.g., intermolecular  $S \rightarrow O$  acetyl migration) were detected, indicating the ultrahigh selectivity and ultrahigh catalytic activity of the neat mGOa catareactors. Thus, 100% conversions and high purities (93–98%) were achieved, as summarized in Table 1. Interestingly, 12 reactants with different kinds of functional groups were tried and successfully transformed into the corresponding thiol compounds, demonstrating the broad functional group tolerance and high selectivity of mGOa catareactors. Moreover, we also tried two macromolecules, epoxy-terminated polydimethylsiloxane (PDMS), and diglycidyl ether bisphenol A (DGEBA), and they were transformed into thiol-terminated ones efficiently, showing the versatility and generality of our mGOa catareactors. Thus, our methodology paves the way for facile synthesis of thiol compounds in large scale.

In particular, for the first time, we accessed thiol compounds with functional groups of  $-\text{Cl}$  (7c),  $-\text{Br}$  (8c), and  $-\text{OH}$  (9c) that cannot be synthesized by the currently reported methods (Scheme 1). In addition, we investigated the kinetics of the model reaction  $7b \rightarrow 7c$  using mGOa as the catalyst. As shown in Figure S56 (Supporting Information), with an increase in the reaction time, the new peak ascribed to  $-\text{SH}$  appears at  $\delta = 1.48$  ppm. At the same time, the peak of H ( $\text{SCOCH}_3$ ) at  $\delta = 2.38$  ppm is gradually weakened. The conversion dependence of the reaction time is linear, reaching 100% conversion at 5 h (Figure 2C).

**Factors and Active Sites Influencing the Catalytic Efficiency.** Why is the performance of mGOa superior to that of other acidic or basic catalysts in catalyzing the acetyl migration reaction? We supposed that this could be attributed

**Table 1. Acetyl Migration Reaction of Latent Thiol Compounds into Thiol Compounds Catalyzed by mGOa Fixed Bed<sup>a</sup>**

Compounds (a)	Time	Products <sup>[b]</sup> (c)	Purity % <sup>[c]</sup>	Conv. <sup>[d]</sup> %
1	8 h		94 (93)	100
2	8 h		95	100
3	6 h		98 (98)	100
4	6 h		97 (94)	100
5	6 h		95	100
6	6 h		95	100
7	5 h		98 (97.5)	100
8	5 h		97	100
9	5 h		97	100
10	6 h		96.5	100
11	6 h		95.7 (93)	100
12	6 h		94 (94)	100
13 <sup>[e]</sup>	8 h		94.9	100
14 <sup>[f]</sup> DGEBA	8 h		97.3	100

<sup>a</sup>Unless otherwise noted, all reactions were performed at room temperature. <sup>b</sup>Unless otherwise noted, the functional group of R stands for CH<sub>3</sub>CO. <sup>c</sup>The purities of products were determined by <sup>1</sup>H NMR spectroscopy; the parts in brackets were confirmed by gas chromatography. <sup>d</sup>Conversion calculated by <sup>1</sup>H NMR spectroscopy. <sup>e</sup>Epoxy-terminated polydimethylsiloxane (PDMS). The structure is shown in Section S1.1, Supporting Information. <sup>f</sup>Diglycidyl ether bisphenol A (DGEBA). The structure is shown in Section S1.1, Supporting Information.

to two main factors: the specific chemical structures of GO and the ultrahigh collision frequency between the reagents and catalytic sites of the GO sheets in the confined space of the microcells. For instance, in a cylindrical catalyst with a diameter of 100 nm, molecule **7b** could collide with the wall at a frequency of  $\nu \times 10^7$  m/s (here  $\nu$  is the velocity of **7b**; m/s) (Figure 1e). In contrast, in a dispersion of individual GO sheets, the collision frequency would be much lower because of their open and free character in solvents. Indeed, control experiments showed that the full conversion from **7b** to **7c** needed 10 h (entry 1 in Table 2), obviously longer than the reaction time (5 h) of being catalyzed by mGOa catareactors.

To assess the active sites presented on GO for the S → O acetyl migration reaction, the composition of the GO was analyzed, and more control experiments were performed, using **7b** → **7c** as the model reaction. As demonstrated by FTIR and X-ray photoelectron spectra (XPS), GO contains C=C bonds and rich oxygen-containing groups—OH, COOH, C—O—C, C=O, and O—C=O—which impart GO possible catalytic sites (Figures 3c, d; S2 in Supporting Information).<sup>20</sup> To speculate on the role of functional groups, we tried different catalysts in the control experiments. In the absence of oxygen-containing functional groups, no product **7c** was found in the reaction system as catalyzed by graphite and graphene nanosheets (entries 2 and 3 in Table 2) exfoliated by the treatment of FeCl<sub>3</sub> and H<sub>2</sub>O<sub>2</sub>, even after 7 days of reaction.<sup>21</sup> A slight conversion (less than 4%) was detected as catalyzed by CCG reduced by N<sub>2</sub>H<sub>4</sub> and HI (entries 4 and 5 in Table 2) with rare functional groups.<sup>22</sup> As a result, it appears that it is the abundant functional groups that work as the catalytic sites, not the conjugated structure, holes, defects, and armchair/zigzag edges.

Basically, the number of OH groups is proportional to the pH value of GO.<sup>23</sup> The effect of pH on the catalysis efficiency was also investigated (entries 6–9 in Table 2). The conversions of GO (pH = 7) and GO (pH = 10) were 15% and 9% as catalyzed by mGOa with pH = 7 and 10 after 10 h of reaction, respectively. These results indicate that protonic functional groups, both —COOH and —OH connected on pi-conjugated carbons,<sup>23</sup> play key roles in such a catalytic reaction. By adding hydrochloric acid into the GO dispersion to adjust the pH (entry 6, Table 2), we afforded acidified mGOa (pH = 3) after freeze-drying. The corresponding conversion of acetyl migration was 57% at 5 h, lower than that of mGOa (pH = 5), likely caused by the stack of GO sheets in the surrounding acid.

Furthermore, we chose isopropyl alcohol, phenol, benzoic acid, anthracene-9-carboxylic acid, and 1-pyrenecarboxylic acid as molecular analogues to mimic the GO catalytic system (entries 10–15 in Table 2). The conversions in all cases were <5% after 10 h of reaction, which in turn revealed that the unique structure of GO, such as ultralarge planar size and unpaired  $\pi$  electrons of carbons at defects, probably made an important contribution to the high catalysis efficiency of GO. We tested the spectrum of electron spin resonance for mGOa. The corresponding line width was ~1 mT, much broader than that of activated carbon, indicating the existence of the unpaired  $\pi$  electrons at the defects/edges of GO (S4.2, Supporting Information).<sup>24</sup>

In addition, we performed control experiments catalyzed by a commercially acidified activated carbon (entry 16, Table 2) with a BET of 800 m<sup>2</sup>/g and pH of 5. The resulting conversion of **7b** → **7c** was very low (11%), which again confirmed the key catalytic role of mGOa was its specific chemical structure.

**Catalyzing Mechanism.** On the basis of the results aforementioned and work of previous researchers,<sup>25</sup> we proposed the reaction mechanism of S → O acetyl migration (Scheme 2). First, thioacetate **A** collides with the protonic functional group of GO (GO—OH), which is activated or polarized by the unpaired  $\pi$  electrons beside it, forming the hybrid of GO-9-membered ring (**B**), via the formation of two hydrogen bonds between GO—OH and **A**. Second, **B** is not stable, and instantly disassociates into 5-membered ring intermediate (**C**) plus GO—OH.<sup>26,27</sup> Finally, the unstable **C** transforms into thiol product **D** immediately. In such a process,

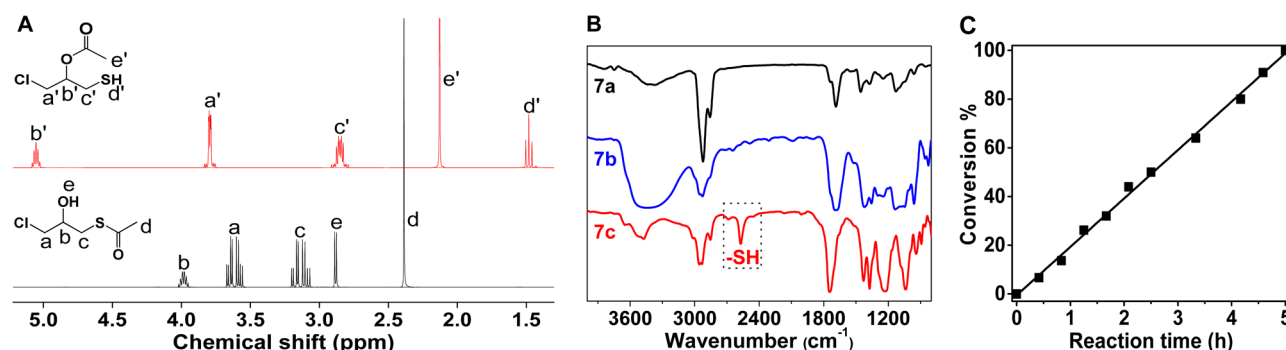
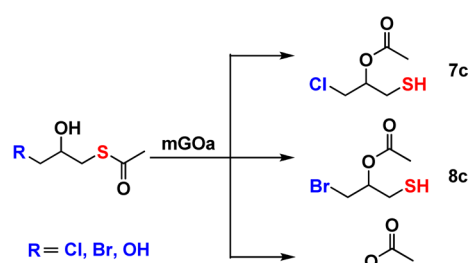


Figure 2. <sup>1</sup>H NMR (A) spectra in CDCl<sub>3</sub> and FTIR spectra (B) of 7a, 7b, and 7c and its kinetics (C) from 7b to 7c.

**Scheme 1. S → O Acetyl Migration Reactions of 7b, 8b, and 9b To Get 7c, 8c, and 9c, Which Cannot Be Synthesized by Currently Reported Methods**



**Table 2. Acetyl Migration Reaction of Latent Thiol Compound 7b into Thiol Compound 7c Catalyzed by Different Catalysts<sup>a</sup>**

Reaction scheme for Table 2: Latent thiol compound 7b (with R = Cl) reacts with mGOa at room temperature (r.t.) to form thiol compound 7c.

entry	catalyst	conversion, % <sup>b</sup>	time
1	GO solution	73	5 h
		100	10 h
2	graphite	0	7 d
3	graphene sheets	0	7 d
4	CCG (N <sub>2</sub> H <sub>4</sub> )	4.0	7 d
5	CCG (HI)	3.1	7 d
6	GO (pH = 3)	57	5 h
7	GO (pH = 5)	100	5 h
8	GO (pH = 7)	15	10 h
9	GO (pH = 10)	9	10 h
10	isopropyl alcohol	0	10 h
11	phenol	4.7	10 h
12	benzoic acid	2.2	10 h
13	cyclohexanecarboxylic acid	1.7	10 h
14	anthracene-9-carboxylic acid	3.7	10 h
15	1-pyrenecarboxylic acid	2.6	10 h
16	acidified activated carbon (pH = 5)	11	10 h

<sup>a</sup>Unless otherwise noted, all reactions were performed at room temperature. <sup>b</sup>Unless otherwise noted, conversion calculated by <sup>1</sup>H NMR spectroscopy.

GO-OH plays the role of catalyst because of its recyclability without any changes of chemical structures. Step I determines the rate of the whole reaction. So the rate in the confined cells is much faster than that in open solution despite with the same

catalyst of GO. Compared with other catalysts of small molecules listed in Table 2, GO shows much higher catalysis efficiency likely because its unpaired  $\pi$  electrons facilitate the easier formation of hybrid B and intermediate C.<sup>28</sup>

**Recyclability of mGOa.** To demonstrate the role of GO as a catalyst rather than as a catalytic reagent, we evaluated the recyclability of mGOa in the model reaction 7b → 7c. After completion of the first reaction, the mGOa could easily be reused in the next reaction by simple elution of the fixed bed with ethyl acetate. After 18 cycles, both the purity (>94%) and yield (~100%) of the product 7c remained constant at the same reaction time (5 h), indicating no decrease in the catalysis efficiency for mGOa after repeated multiple uses (Figure 4 and Figure S38–55, Supporting Information). Significantly, we characterized mGOa used for 18 times by FTIR, thermogravimetric analysis (TGA), XPS, and Raman (Figure 3), and no differences in the chemical structures or composition compared with a fresh sample were found. These powerful results demonstrate that mGOa does act as a catalyst in this organic reaction. It was reported that GO could catalyze the oxidation of thiols to form sulfoxides at a high temperature of 100 °C.<sup>29</sup> In our case, the reactions were carried out at room temperature, no any sulfoxides were detected in our catalysis system, showing the high catalytic selectivity of our mGOa catareactors.

## CONCLUSION

We fabricated mGOa built with microcells. For the first time, such a mGOa was used as a fixed bed carbocatalyst without loading extra catalytic compounds. Our mGOa integrates both the advantages of easy purification of the products associated with a conventional fixed bed catalytic reactor and the high catalysis efficiency of reactors. The GO-constructed cell plays both roles of reactor and catalyst, which we consequently coined as a catareactor. The macroscopic catareactors showed ultrahigh catalysis efficiency (100% conversion at 5–8 h) and selectivity (100%) at rt for the model reaction of S → O acetyl migration based on the protonic functional groups, ultralarge size, and unpaired electrons of GO, thus opening the door to facile and scalable production of thiol compounds and thiol-terminated polymers. The acidic character of GO enabled us to first achieve thiol compounds with halogen atoms and hydroxyl groups. Because of the “cage effect” in the confined space, the macroscopic catareactors showed a 2-fold higher catalysis efficiency than the GO dispersions. The macroscopic catareactors are robust enough to be recycled without decreasing the catalytic activity, even after recycling up to 18 times. The advantages of a high catalytic efficiency, high selectivity, high recyclability, simple purification of products,

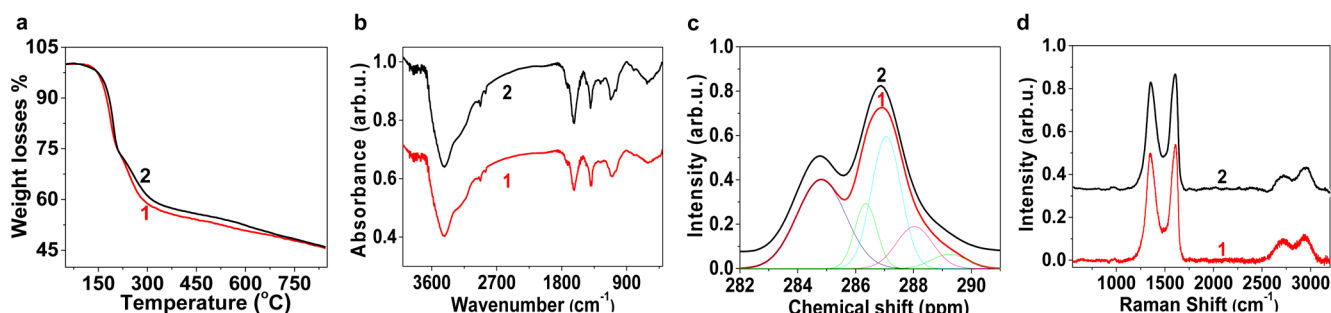


Figure 3. Comparison of the mGOa before (1) and after (2) being reused 18 times by (a) TGA plots, (b) IR spectra, (c) XPS spectra, and (d) Raman spectra.

## Scheme 2. Structural Model of mGOa Catareactor and Its Catalytic Mechanism of S → O Acetyl Migration in a Confined Cell

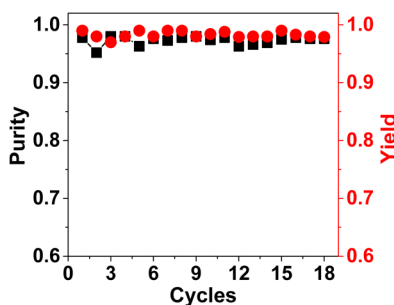
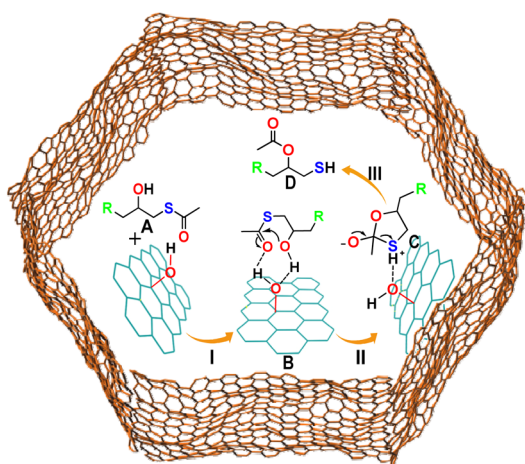


Figure 4. Reusability of mGOa fixed-bed in catalyzing the acetyl migration reaction from **7b** to **7c** measured by GC (Figure S38–55 and Table S1, Supporting Information).

and tolerance to various polar and apolar functional groups are integrated onto one catalyst of mGOa, highlighting the design of novel carbocatalysts and fixed bed catalytic reactors.

## ■ ASSOCIATED CONTENT

### Supporting Information

The Supporting Information is available free of charge on the ACS Publications website at DOI: 10.1021/acscatal.5b00233.

Detailed experimental procedures as well as corresponding analytical and spectral characterization data (PDF)

## ■ AUTHOR INFORMATION

### Corresponding Author

\*E-mail: chaogao@zju.edu.cn.

### Notes

The authors declare no competing financial interest.

## ■ ACKNOWLEDGMENTS

This work was supported by the National Natural Science Foundation of China (nos. 21325417 and 51173162) and China Postdoctoral Science Foundation (2014M551724).

## ■ REFERENCES

- (1) (a) Navalon, S.; Dhakshinamoorthy, A.; Alvaro, M.; Garcia, H. *Chem. Rev.* **2014**, *114*, 6179–6212. (b) Jana, R.; Pathak, T. P.; Sigman, M. S. *Chem. Rev.* **2011**, *111*, 1417–1492.
- (2) (a) Novoselov, K. S.; Geim, A. K.; Morozov, S. V.; Jiang, D.; Zhang, Y.; Dubonos, S. V.; Grigorieva, I. V.; Firsov, A. A. *Science* **2004**, *306*, 666–669. (b) Novoselov, K. S.; Geim, A. K.; Morozov, S. V.; Jiang, D.; Katsnelson, M. I.; Grigorieva, I. V.; Dubonos, S. V.; Firsov, A. A. *Nature* **2005**, *438*, 197–200. (c) Rao, C. N. R.; Sood, A. K.; Subrahmanyam, K. S.; Govindaraj, A. *Angew. Chem., Int. Ed.* **2009**, *48*, 7752–7777.
- (3) (a) Stengl, V.; Popelkova, D.; Vlácil, P. *J. Phys. Chem. C* **2011**, *115*, 25209–25218. (b) Meng, Q. Y.; Zhong, J. J.; Liu, Q.; Gao, X. W.; Zhang, H. H.; Lei, T.; Li, Z. J.; Feng, K.; Chen, B.; Tung, C. H.; Wu, L. Z. *J. Am. Chem. Soc.* **2013**, *135*, 19052–19055.
- (4) (a) Liu, M. M.; Lu, Y. Z.; Chen, W. *Adv. Funct. Mater.* **2013**, *23*, 1289–1296. (b) Sun, Z. P.; Zhang, W. Q.; Lu, X. M. *Adv. Mater. Res.* **2012**, *535–537*, 1467–1477.
- (5) (a) Chen, Y.; Ho, D. M.; Lee, C. *J. Am. Chem. Soc.* **2005**, *127*, 12184–12185. (b) Wang, Y.; Wang, X.; Antonietti, M. *Angew. Chem., Int. Ed.* **2012**, *51*, 68–89. (c) Leitner, W. *Science* **1999**, *284*, 1780–1781.
- (6) (a) Rourke, J. P.; Pandey, P. A.; Moore, J. J.; Bates, M.; Kinloch, I. A.; Young, R. J.; Wilson, N. R. *Angew. Chem., Int. Ed.* **2011**, *50*, 3173–3177. (b) He, W. H.; Lu, L. H. *Adv. Funct. Mater.* **2012**, *22*, 2542–2549.
- (7) (a) Hou, X. L.; Li, J. L.; Drew, S. C.; Tang, B.; Sun, L.; Wang, X. G. *J. Phys. Chem. C* **2013**, *117*, 6788–6793. (b) Ivanciuc, O.; Klein, D. J.; Bytautas, L. *Carbon* **2002**, *40*, 2063–2083. (c) Feng, R. C.; Zhou, W.; Guan, G. H.; Li, C. C.; Zhang, D.; Xiao, Y. N.; Zheng, L. C.; Zhu, W. X. *J. Mater. Chem.* **2012**, *22*, 3982–3989.
- (8) Tang, Z. H.; Shen, S. L.; Zhuang, J.; Wang, X. *Angew. Chem., Int. Ed.* **2010**, *49*, 4603–4607. (b) Su, C.; Tandiana, R.; Balapanuru, J.; Tang, W.; Pareek, K.; Nai, C. T.; Hayashi, T.; Loh, K. P. *J. Am. Chem. Soc.* **2015**, *137*, 685–690.
- (9) Dreyer, D. R.; Bielawski, C. W. *Chem. Sci.* **2011**, *2*, 1233–1240.
- (10) (a) Dreyer, D. R.; Jia, H.-P.; Todd, A. D.; Geng, J.; Bielawski, C. W. *Org. Biomol. Chem.* **2011**, *9*, 7292–7295. (b) Dreyer, D. R.; Jia, H. P.; Bielawski, C. W. *Angew. Chem., Int. Ed.* **2010**, *49*, 6686–6686. (c) Dreyer, D. R.; Jarvis, K. A.; Ferreira, P. J.; Bielawski, C. W. *Polym. Chem.* **2012**, *3*, 757–766.

- (11) Long, Y.; Zhang, C. C.; Wang, X. X.; Gao, J. P.; Wang, W.; Liu, Y. *J. Mater. Chem.* **2011**, *21*, 13934–13941.
- (12) (a) Hoyle, C. E.; Lowe, A. B.; Bowman, C. N. *Chem. Soc. Rev.* **2010**, *39*, 1355–1387. (b) Hoyle, C. E.; Bowman, C. N. *Angew. Chem., Int. Ed.* **2010**, *49*, 1540–1573.
- (13) Cremllyn, R. J. W. *An Introduction to Organosulfur Chemistry*; Wiley: New York, 1996.
- (14) (a) White, S. R.; Moore, J. S.; Sottos, N. R.; Krull, B. P.; Santa Cruz, W. A.; Gergely, R. C. R. *Science* **2014**, *344*, 620–623. (b) Chen, X.; Zhou, Y.; Peng, X.; Yoon, J. *Chem. Soc. Rev.* **2010**, *39*, 2120–2135.
- (15) (a) Tretyakov, Y. D.; Lukashin, A. V.; Eliseev, A. A. *Usp. Khim.* **2004**, *73*, 974–998. (b) Xu, Y.; Sheng, K.; Li, C.; Shi, G. *ACS Nano* **2010**, *4*, 4324–4330. (c) Zhang, X.; Sui, Z.; Xu, B.; Yue, S.; Luo, Y.; Zhan, W.; Liu, B. *J. Mater. Chem.* **2011**, *21*, 6494–6497.
- (16) (a) Abbasi, M. *Tetrahedron Lett.* **2012**, *53*, 3683–3685. (b) Wang, G.; Peng, L.; Zheng, Y.; Gao, Y.; Wu, X.; Ren, T.; Gao, C.; Han, J. *RSC Adv.* **2015**, *5*, 5674–5679.
- (17) (a) Xu, Z.; Gao, C. *ACS Nano* **2011**, *5*, 2908–2915. (b) Xu, Z.; Sun, H. Y.; Zhao, X. L.; Gao, C. *Adv. Mater.* **2013**, *25*, 188–193.
- (18) Sun, H. Y.; Xu, Z.; Gao, C. *Adv. Mater.* **2013**, *25*, 2554–2560.
- (19) Yang, Y.; Liu, X.; Li, X. B.; Zhao, J.; Bai, S. Y.; Liu, J.; Yang, Q. H. *Angew. Chem., Int. Ed.* **2012**, *51*, 9164–9168.
- (20) Kobayashi, Y.; Fukui, K. -i.; Enoki, T.; Kusakabe, K. *Phys. Rev. B: Condens. Matter Mater. Phys.* **2006**, *73*, 125415.
- (21) Geng, X. M.; Guo, Y. F.; Li, D. F.; Li, W. W.; Zhu, C.; Wei, X. F.; Chen, M. L.; Gao, S.; Qiu, S. Q.; Gong, Y. P.; Wu, L. Q.; Long, M. S.; Sun, M. T.; Pan, G. B.; Liu, L. W. *Sci. Rep.* **2013**, *3*, 1134.
- (22) Murugan, A. V.; Muraliganth, T.; Manthiram, A. *Chem. Mater.* **2010**, *22*, 2692–2692.
- (23) Dimiev, A.; Kosynkin, D. V.; Alemany, L. B.; Chaguine, P.; Tour, J. M. J. *Am. Chem. Soc.* **2012**, *134*, 2815–2822.
- (24) (a) Enoki, T.; Takai, K. *Solid State Commun.* **2009**, *149*, 1144–1150. (b) Joly, V. L. J.; Takahara, K.; Takai, K.; Sugihara, K.; Enoki, T.; Koshino, M.; Tanaka, H. *Phys. Rev. B: Condens. Matter Mater. Phys.* **2010**, *81*, 115408.
- (25) Pavlova, L.; Rachinskii, F. Y. *Russ. Chem. Rev.* **1968**, *37*, 587.
- (26) (a) Sjöberg, B. *Ber. Dtsch. Chem. Ges. B* **1942**, *75*, 13–29. (b) Miles, L. W. C.; Owen, L. N. *J. Chem. Soc.* **1952**, 817–826. (c) Ward, J. P. *Chem. Phys. Lipids* **1988**, *47*, 217–224.
- (27) Martin, R. B.; Hedrick, R. I. *J. Am. Chem. Soc.* **1962**, *84*, 106–110.
- (28) (a) Matsuki, Y.; Maly, T.; Ouari, O.; Karoui, v.; Le Moigne, F.; Rizzato, E.; Lyubenova, S.; Herzfeld, J.; Prisner, T.; Tordo, P.; Griffin, R. G. *Angew. Chem., Int. Ed.* **2009**, *48*, 4996–5000. (b) Su, C. L.; Acik, M.; Takai, K.; Lu, J.; Hao, S. J.; Zheng, Y.; Wu, P. P.; Bao, Q. L.; Enoki, T.; Chabal, Y. J.; Loh, K. P. *Nat. Commun.* **2012**, *3*, 1298.
- (29) Dreyer, D. R.; Jia, H. P.; Todd, A. D.; Geng, J. X.; Bielawski, C. W. *Org. Biomol. Chem.* **2011**, *9*, 7292–7295.